ORGANIC PROCESS RESEARCH & DEVELOPMENT
OPR&D

Full Paper

Development of a Zinc-Mediated Approach to a 2,3-cis-pyrrolidine Arginase Inhibitor

Thomas W Lyons, Theodore Martinot, Cyndi He, Ji Qi, and Guangxin Shao

Org. Process Res. Dev., **Just Accepted Manuscript** • DOI: 10.1021/acs.oprd.0c00171 • Publication Date (Web): 09 Jun 2020

Development of a Zinc-Mediated Approach to a 2,3-*cis*-pyrrolidine Arginase Inhibitor

Thomas W. Lyons[*†], *Theodore A. Martinot*[†‡], *Cyndi Qixin He*[◊], *Ji Qi*[◦], *Guangxin Shao*[□]

AUTHOR ADDRESS [†]Department of Process Research and Development, Merck & Co., Inc., 33 Avenue Louis Pasteur, Boston, MA 02115, USA. [◊] Department Modeling and Informatics, Merck & Co., Inc., 90 E. Scott Ave., Rahway NJ 07065, USA. [◦]Department of Process Research and Development, Merck &Co., Inc., 126 E. Lincoln Ave, Rahway NJ 07065, USA. [□] Department of Synthetic Chemistry, Pharmaron Beijing Co., Ltd. 6 Taihe Rd BDA, Beijing, 100176, China.

Table of Contents Figure

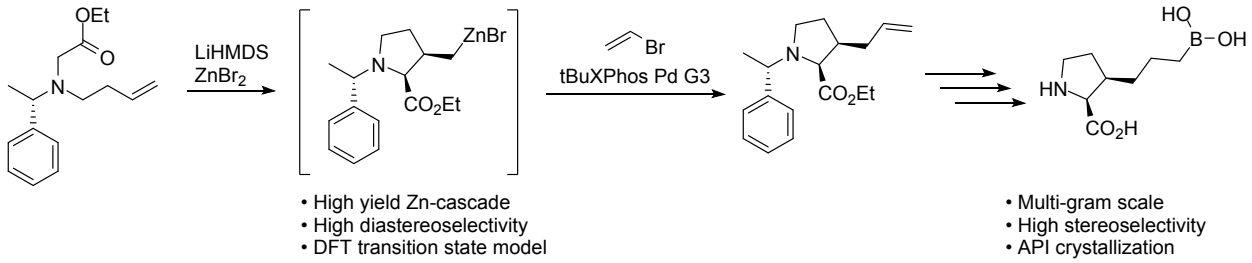

- High yield Zn-cascade
- High diastereoselectivity
- DFT transition state model

- Multi-gram scale
- High stereoselectivity
- API crystallization

Abstract

This manuscript outlines the development activities toward a robust synthesis of a *cis*-2,3-pyrrolidine via a tandem zinc-enolate cyclization / Negishi coupling that proceeds with high diastereoselectivity. The methodology facilitated a gram-scale delivery of the target API and eliminated the need for costly chiral resolutions and inefficient protecting group manipulations. A series of DFT experiments provided a transition state model that agrees closely with the experimental observations and provides a more in-depth understanding of the observed selectivity.

KEYWORDS. Arginase inhibitor, zinc, cyclization, Negishi

Introduction

Arginase is a manganese-containing enzyme that catalyzes the hydrolysis of L-arginine to L-ornithine and urea as part of the urea cycle. In humans, this enzyme is predominantly found in the liver (ARG I, hepatic arginase), but has also been found within the

mitochondrial matrix (ARG II, extrahepatic arginase).[1-3] By regulating the availability of L-arginine and L-ornithine, arginase plays an important role in the cellular function of both normal and cancer cells.[4] High levels of arginase activity have been reported in various types of cancer including breast,[5] pancreatic,[6] non-small cell lung,[7] and prostate cancers.[8] Several studies have identified a promising therapeutic link between this metabolic pathway and cancer.[9, 10] Moreover, small molecule arginase inhibitors have been shown to have significant immune-mediated anti-tumor effects.[11, 12] In particular, the combination of arginase inhibitors with checkpoint inhibitors in mice has led to a decrease in tumor growth.[12] Given these studies and related reports, arginase has become an attractive target for cancer therapy.

First Generation Synthesis

As part of a drug discovery program we became interested in robust methods for the synthesis of compound **7** as an arginase inhibitor to support exploratory safety and toxicity studies. Initial quantities of **7** were produced via the pyrrole functionalization strategy shown in Scheme 1. This route utilized a Stille[13] coupling of an advanced intermediate **1**[14,15] with allyl tin, followed by an Ir-catalyzed hydroboration of the resulting allyl chain to

give **3**. Subsequent hydrogenation of the heterocycle and Boc cleavage revealed (+/-) **5**. Cbz protection of (+/-) **5** was required to achieve efficient supercritical fluid chromatography (SFC) separation of the enantiomers of **6**. Finally, global deprotection with HCl and ion exchange chromatography (IEC) produced **7** as a white powder after lyophilization.[16, 17] While this sequence was suitable for small-scale preparation (< 1g) of **7** and related derivatives, it was plagued by low yields and an SFC separation which necessitated a protecting group change. To alleviate these constraints and provide more efficient access to **7** we began exploring alternative approaches to the *cis*-2,3-disubstituted proline core.[18, 19]

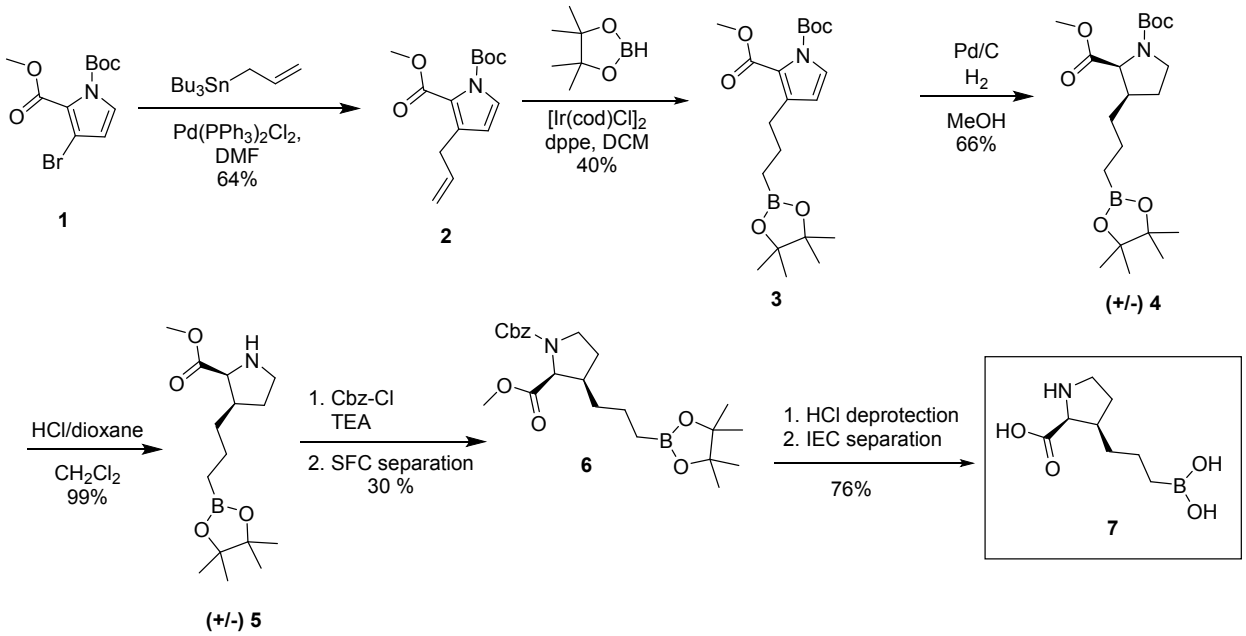

Scheme 1. Initial route to **7**

We envisioned a different synthetic sequence, outlined in Scheme 2, that leveraged the amino-zinc-enolate cyclization reported by Karoyan and Chassaing[20-22] simultaneously with others[23-25] to provide access to the desired *cis*-3-allyl pyrrolidine product **9**. This would involve a Zn-mediated cyclization, followed by an in situ Negishi coupling to afford the allyl product. This new route provides three key advantages. First, the starting material is inexpensive and readily synthesized from commercial compounds. Second, the benzylamine chiral auxiliary provides stereocontrol and obviates the need for SFC separation. Third, the overall step count is reduced, increasing the efficiency of the synthesis.

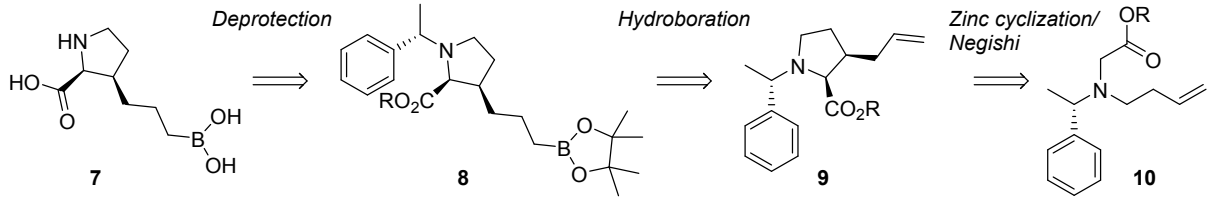

Scheme 2. Retrosynthetic Analysis

While the zinc cyclization had been carried out with a number of electrophiles[22, 26, 27, 28], the in situ Negishi sequence had only been demonstrated with iodobenzene[29, 30]; the use of vinyl halides has not been reported. Dialkylbiarylphosphine ligands such as CPhos

have been shown to be highly effective in the cross-coupling of alkylzinc reagents.[31, 32] Thus we began exploring Negishi conditions with that ligand system. We were pleased to see our initial conditions of 10 mol % CPhos Pd G4 with 1.5 equivalents vinyl bromide provided 35% isolated yield of the desired product (Scheme 3). The crude ^{1}H NMR spectrum indicated an approximately 87:13 ratio of diastereomers. Column chromatography and further 2D ^{1}H NMR analysis confirmed that the major diastereomer bore the desired *cis*-2,3 configuration.[33] With this exciting proof-of-concept in hand, we set about optimizing this reaction.

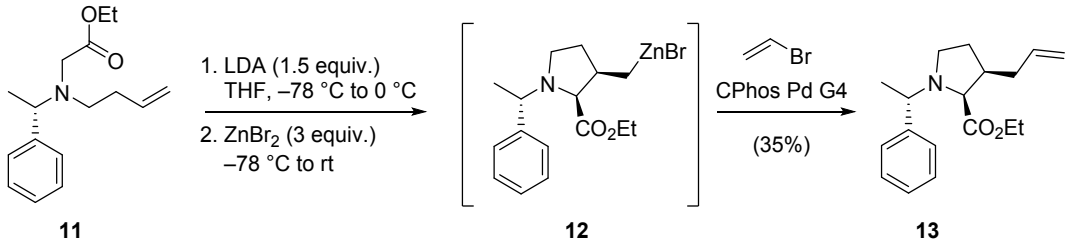

Scheme 3. One Pot Zn-Mediated Cyclization.

Zinc-Cyclization Optimization. To further our understanding of this key transformation we focused on the first cyclization step by quenching the Zn reaction with water rather than adding a Pd/vinyl bromide solution. This afforded the methyl pyrrolidine product and the opportunity to interrogate the effects of base, solvent, and ester identity on the

cyclization. To that end, we examined several organic bases in THF. Our initial base choice based on literature precendent[21] was LDA and provided high conversion and dr. LiHMDS and KHMDS also provided high conversion to the desired product (R=Et, Table 1, entries 2, 3). The stronger base *n*BuLi (Table 1, entry 4) led to consumption of **11a**, but was ultimately deleterious to the formation of **14a**. The weaker alkoxide bases (Table 1, entries 5, 7, 8) were ineffective, leaving residual **11a** to be observed in the LCMS. Taken together, these data suggest the alkoxide bases are unable to generate the enolate sufficiently and *n*BuLi is too strong a base, which leads to decomposition.

We also explored other etherial solvents in these reactions including diethyl ether, and diisopropyl ether. While initial experiments with diethyl ether showed promising conversions and dr (e.g. Table 1, entry 10), we found these results to be difficult to reproduce in repeat experiments and ultimately not compatible with the Negishi conditions. A larger scale of this reaction revealed a biphasic mixture upon addition of the $ZnBr_2$ solution and warming to 0 °C. This mixture became gelatinous in appearance over time and was ultimately deleterious to the reaction, resulting in low yield of the desired Negishi product.[34] Other common etherial solvents including 2-Me-THF, diisopropyl ether,

and CPME resulted in minimal conversion (>10%) and were unsuitable for the Negishi conditions.

Interestingly, the choice of ester had a strong influence on the outcome of the reaction. The benzyl ester substrate **11b** (R=Bn, entries 11-14) provided lower conversion and lower dr relative to **11a** (R=Et). Switching to the tBu ester **11c** (R=tBu, entries 15, 16) provided only trace conversion to the desired product, leaving predominantly residual starting material. In the end, LiHMDS in THF using R=Et provided the most robust conversion and dr for this reaction, which improved slightly at larger scale; a reaction run on a 5 g scale gave 95% conversion and 87:13 dr of **14a**.

Table 1. Base and Substrate Screen for the Cyclization Reaction [a]

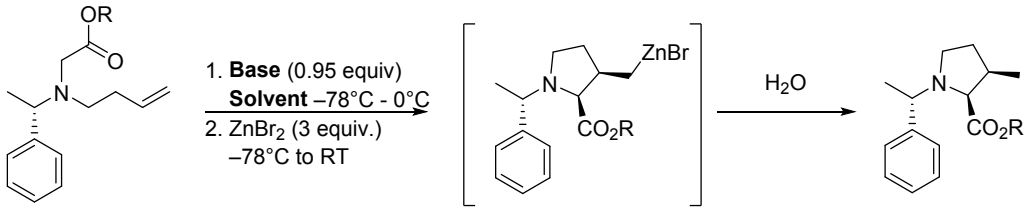

11 a-c **12 a-c** **14 a-c**

Entry	Base	R	Solvent	Conversion %	dr
1	LDA	Et (**11 a**)	THF	82	92:8

2	LiHMDS	Et	THF	91	87:13
3	KHMDS	Et	THF	98	83:17
4	nBuLi	Et	THF	83	n/a
5	LiOtBu	Et	THF	1.2	0
6	LiTMP	Et	THF	91	85:15
7	NaOtBu	Et	THF	<5	n/a
8	KOtBu	Et	THF	<5	n/a
9	LDA	Et	Et_2O	78	92:8
10	LiHMDS	Et	Et_2O	94	93:7
11	LDA	Bn (**11 b**)	THF	55	83:17
12	LDA	Bn	Et_2O	61	75:25
13	LiHMDS	Bn	THF	56	83:17
14	LiHMDS	Bn	Et_2O	65	75:25
15	LDA	tBu (**11 c**)	THF	<5	n/a
16	LDA	tBu	Et_2O	<5	n/a

[a] Reaction conversion and dr determined on the basis of the LCAP of the desired product from the crude reaction mixture. $ZnBr_2$ added as a solid to the reaction mixture.

Using the optimized conditions, we monitored this reaction using in situ IR (ReactIR) which illustrate the steps of the cyclization. As shown in Figure 1, addition of LiHMDS leads to rapid formation of the Li-enolate. The disappearance of the ester peak at 1752 cm^{-1} is followed by formation of a new peak at 1663 cm^{-1}. Addition of $ZnBr_2$ then produces

the proposed Zn-enolate characterized by a new shift in the IR spectrum to 1680 cm^{-1} and shown below in the calculated *Z*-geometry (Figure 1). Conversion to the cyclized intermediate takes place over several hours at –78 °C as indicated by the disappearance of enolate IR signal and formation of the new alkyl-Zn species **12** in the IR spectrum (Figure 1). Closely monitoring the formation of the cyclized intermediate **12** via ReactIR or LCMS enabled high conversion in the subsequent Negishi coupling upon scale-up.

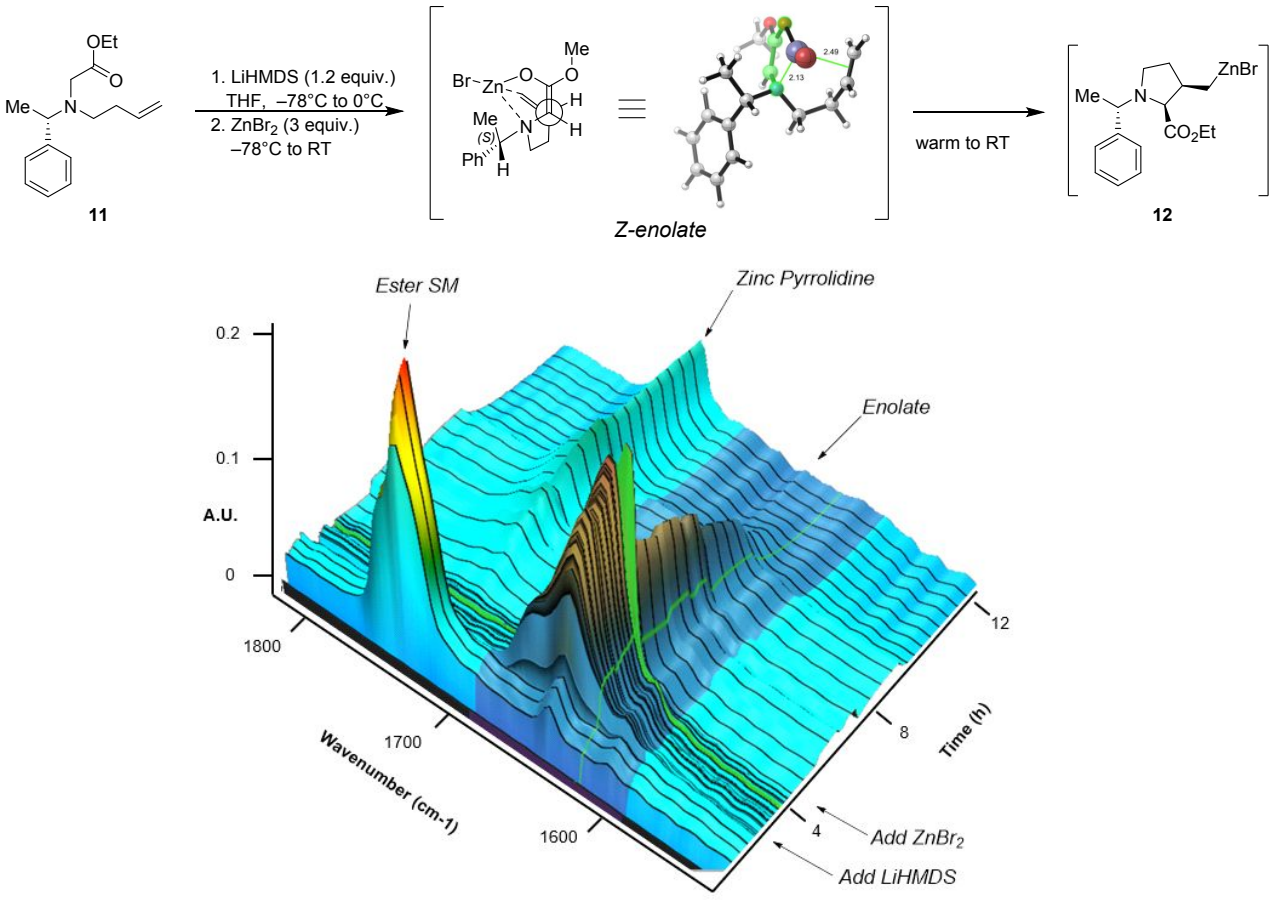

Figure 1. Following the cyclization reaction using ReactIR

Negishi Reaction Optimization. While our initial result with CPhosPd G4[31] provided rapid and clean conversion to the desired allyl pyrrolidine, we were interested in exploring catalyst alternatives that were less expensive and more amenable to larger scale. Thus, we pursued an extensive screen of known Pd precatalysts in our coupling conditions using a freshly prepared solution of the alkyl-Zn species. While the complexities of distributing this zinc solution into micro vial kits resulted in lower overall conversions than larger scale reactions[35], the observed relative performance from the data provided an adequate guide for appropriate alternatives (Figure 2). These results indicated that a number of viable replacements for CPhosPd G4 existed, including APhos G2, DTBPF G3, and tBuXPhos G3. While several Pd precatalysts were competent for this transformation, we found the cost and ready availability of tBuXPhos to be the most appealing choice. In addition to catalyst, the high conversion to the cyclized Zn intermediate **12** was also critical in achieving high yields of **13**, highlighting the importance of in situ monitoring.

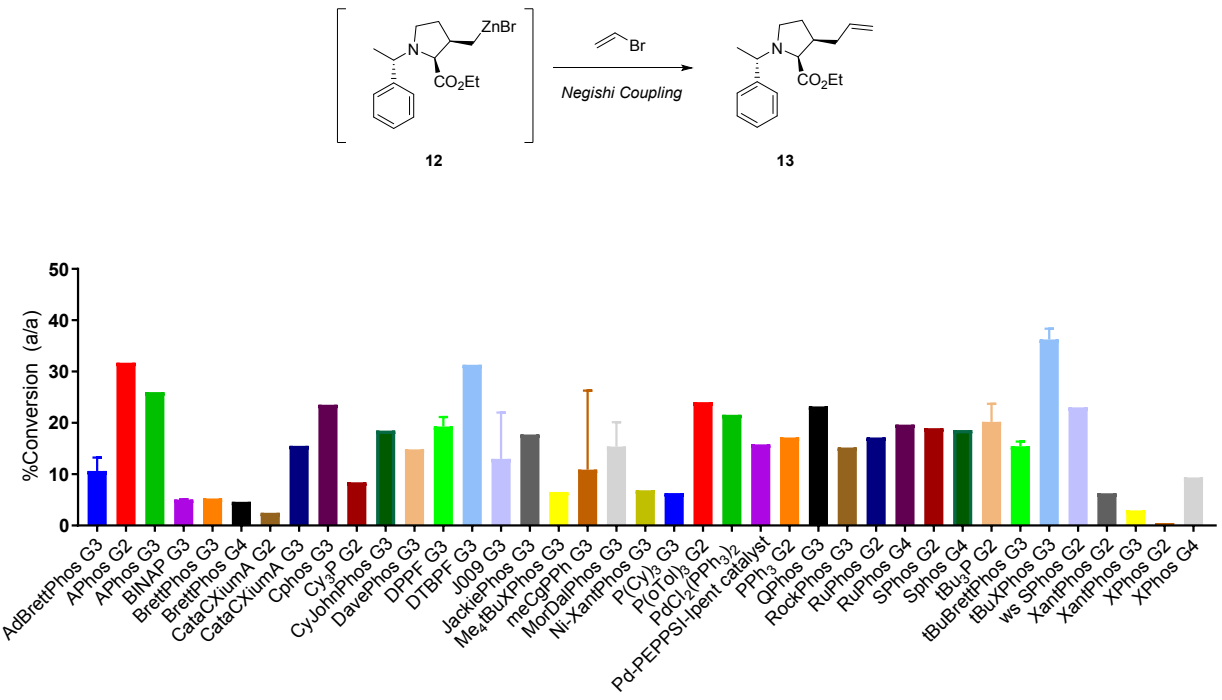

Figure 2. Investigation of 39 ligand-supported precatalysts for Negishi coupling. Error bars represent conversion measured over two experiments.

Computational Analysis. To gain insight into the nature of the reaction selectivity, we undertook a series of DFT experiments that provided a transition state model for the Zn-mediated cyclization.[36] In the cyclization step, two new stereocenters are generated in the C–C bond formation, leading to four possible diastereomeric pathways in the presence of the existing chirality from the auxiliary (Figure 3). Initial conformational analysis showed that to access the *trans*-ring product, an *E* configuration of the amino

zinc enolate is adopted to coordinate to the enolate oxygen and the terminal alkene, giving rise to the (*S*,*S*,*S*)- and (*S*,*R*,*R*)-pyrrolidine products. The *cis*-products, on the other hand, comes from a *Z*-enolate, where both the enolate oxygen and the nitrogen are on the same side and can coordinate to zinc.

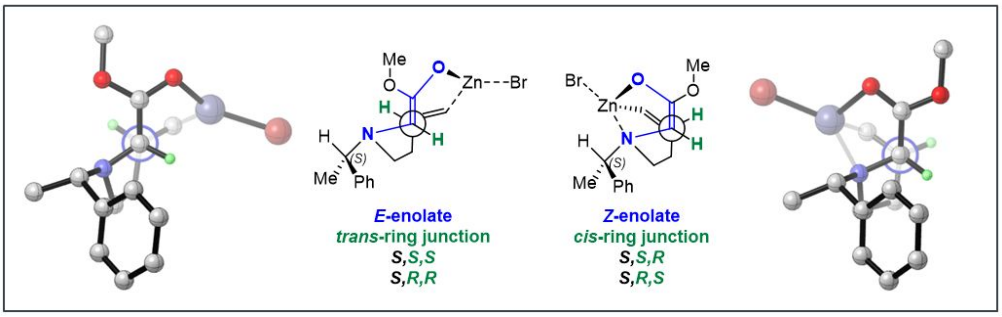

Figure 3. Possible diastereomeric pathways of Zn-mediated cyclization and DFT-optimized transition states of tetrahedral zinc complexes.

The reaction energy profiles for 4-coordinate (tetrahedral) and 6-coordinate (octahedral) zinc were explored. Previous DFT studies have shown that zinc prefers to be tetrahedral in the gas-phase, octahedral in aqueous solution, and can adopt either geometry in a protein environment depending on the type of ligand and solvent accessibility.[37] Figure 4 shows the lowest energy tetrahedral and octahedral zinc complexes undergoing cyclization to the corresponding *cis*- and *trans*- products. In both models, the *Z*-enolate

12a′-*Z* is significantly more stable ($\Delta\Delta G$ = 20 kcal/mol) than the *E* isomer **12a′-*E***. This large energy difference partly arises from the absence of nitrogen and alkene coordination to zinc in the *E*-enolate, because the enolate oxygen and the nitrogen are *trans* to each other and cannot simultaneously coordinate to zinc. To account for the empty coordination sites, explicit ether molecules are included in the *E*-enolate pathway.[38] Comparing the *cis*-/*trans*-determining transition states, formation of the 2,3-*trans* product is highly disfavored ($\Delta\Delta G^{\ddagger}$ = 11–18 kcal/mol) in both coordination models.

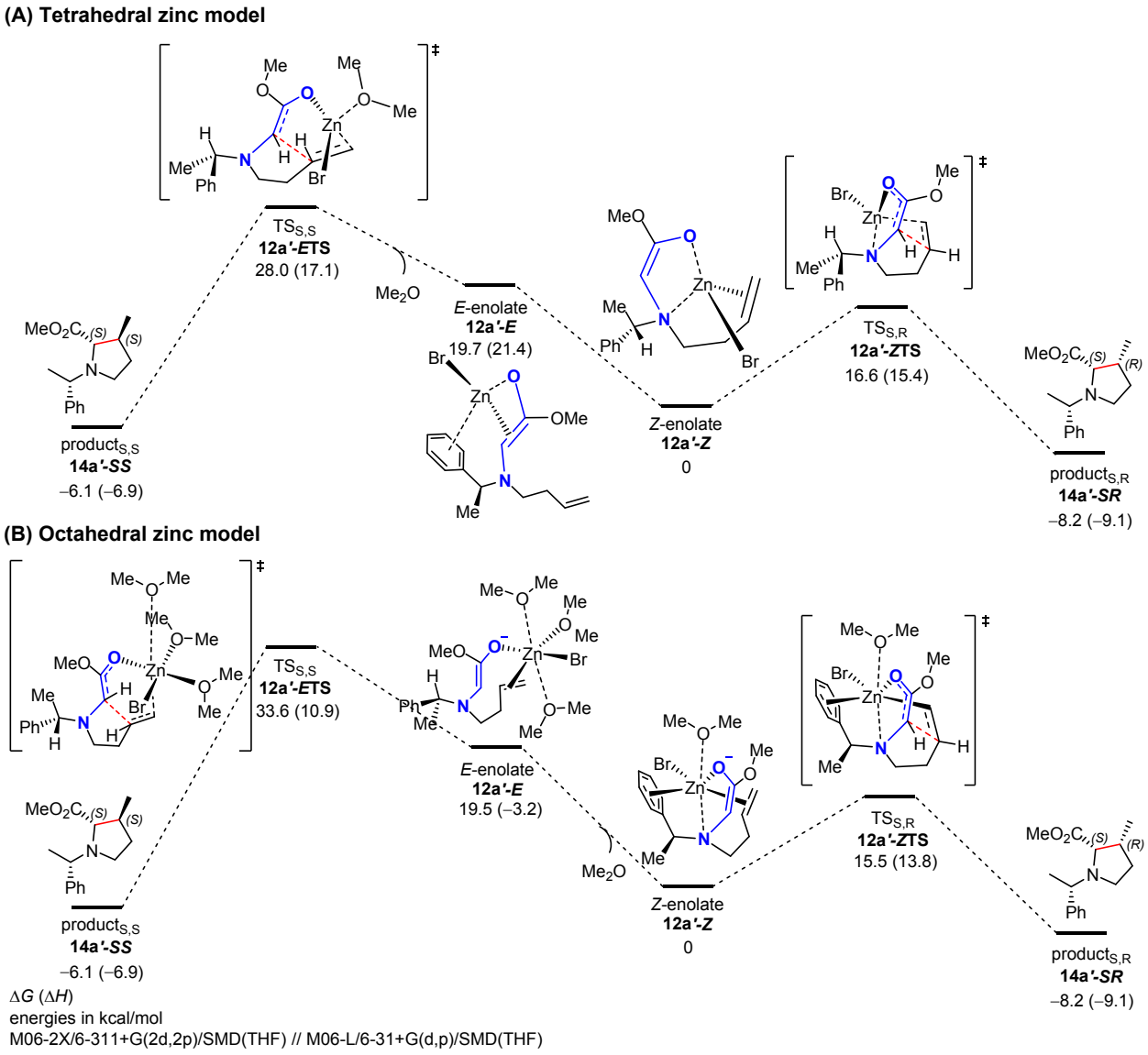

Figure 4. Calculated cyclization reaction energy profiles of (A) tetrahedrally and (B) octahedrally coordinated zinc complexes. (TS = transition state).

A closer examination of the two possible transition states leading to *cis-(2S,3R)*- and *cis-(2R,3S)*-products reveals a 0.8 kcal/mol difference in energy between the two

diastereomeric TSs (Figure 5). A fine balance of two key interactions, the favorable phenyl–zinc coordination and the methyl–methylene repulsion (Figure 5, green line), dictate diastereoselectivity. A similar **12a′-TS**$_{Z,S,R}$ is predicted to be 0.8 kcal/mol more stable than **12a′-TS**$_{Z,R,S}$. These data match nicely with the experimental diastereomeric ratio of 87:13 and no observable amount of the 2,3-*trans* product. These interactions are also in agreement with previously proposed transition state models[22, 24] and the reported loss of dr when the phenyl-zinc interaction is replaced with a cyclohexyl ring.[24] Additionally, in both TSs, the methoxy group of the ester points away from the chiral auxiliary (Figure S1). The computed dr of benzyl and tert-butyl esters are consistent with experimental observations that varying the ester does not increase *cis*-(*S,R*)/(*R,S*)-selectivity (Figure 3). This suggests that enolate formation rather than cyclization is the problematic step in our optimization reactions (Table 1, entries 11-14). Interestingly, while both the tetrahedral and octahedral zinc models give reasonable and surmountable energy barriers ($\Delta G^{\ddagger}$ = 15–16 kcal/mol), the former predicts the wrong *cis*-diastereoselectivity (Figure S1, S2), which suggests that an octahedrally coordinated zinc complex is more likely the operable species.

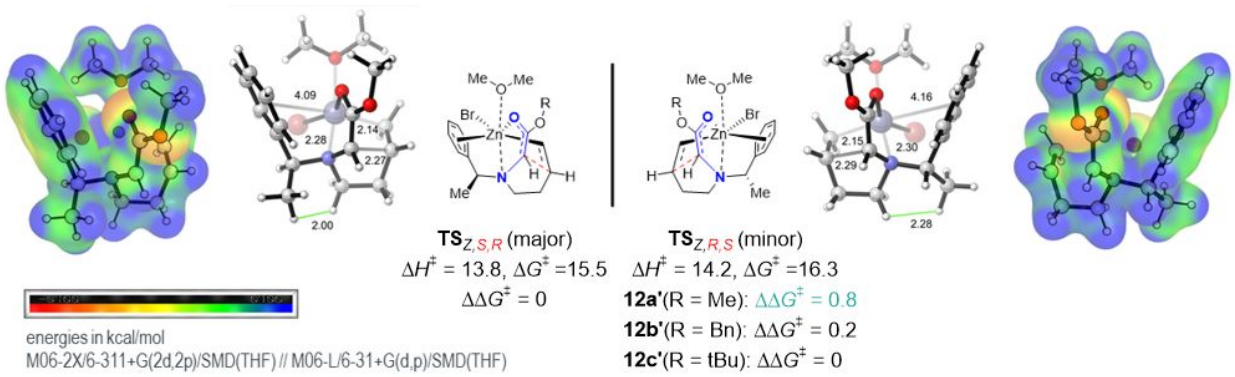

Figure 5. Proposed role of chiral auxiliary in the diastereoselectivity of two possible *cis*-products.

Optimized Route. The final route provided us with a good yield of **7** and a high level of purity for toxicity studies (Scheme 4). It began with the nucleophilic displacement of 4-bromobutene (**15**) with (*S*)-methylbenzylamine, an inexpensive source of chirality for this sequence. The homoallylamine **16** was exposed to the bromoester in the presence of base to yield the cyclization precursor (**11**) in 85% yield. Subjecting **11** to the optimized conditions of LiHMDS and $ZnBr_2$ in THF gave >90% conversion to the alkyl-Zn intermediate. Addition of vinyl bromide and tBuXPhos Pd G3 to the mixture gave the desired allyl pyrrolidine **13** in 76% isolated yield, and this reaction was successfully scaled

to >200 g. Purity upgrade of the desired cis-diastereomer was achieved by crystallization of the HCl salt (**17**) in toluene. Attempts were made to carry out this crystallization directly from the reaction mixture but were ultimately less efficient than the isolation from toluene. In addition to affording a diastereomeric enrichment of the reaction product, the isolation of the HCl salt **17** provided a practical crystalline handle in the synthetic sequence among intermediates that otherwise had poor physical properties. An important challenge in the synthesis of **7** and related compounds is that intermediates were often oils that could only be purified using chromatography. Thus, any opportunity to capitalize on key crystalline intermediates for impurity control provided a significant benefit.[39] While the HCl salt could be used directly in the subsequent coupling, a lower overall conversion was observed compared to the free base. Therefore, the free base **13** was generated with $NaHCO_3$ and subsequently subjected to Ir-catalyzed borylation with HBPin to give **18** in 68% yield. Lower iridium catalyst loading can be employed, but this resulted in longer reaction times and greater amounts of boronic ester hydrolysis – the major side product of this reaction. Hydrogenation with $Pd(OH)_2$ cleaved the benzyl group and resulted in partial deprotection of the boronic acid to give a mixture of **19** and **20**. Subjecting this mixture to HCl at 80 °C

gave full deprotection of the desired compound, which was subsequently purified via ion-exchange chromatography. Importantly, we have also found crystallization conditions for **7** from IPA/H_2O, which were suitable for purging any residual **20** remaining in the reaction. These crystallization conditions may be suitable for related compounds, which have been historically difficult to purify.

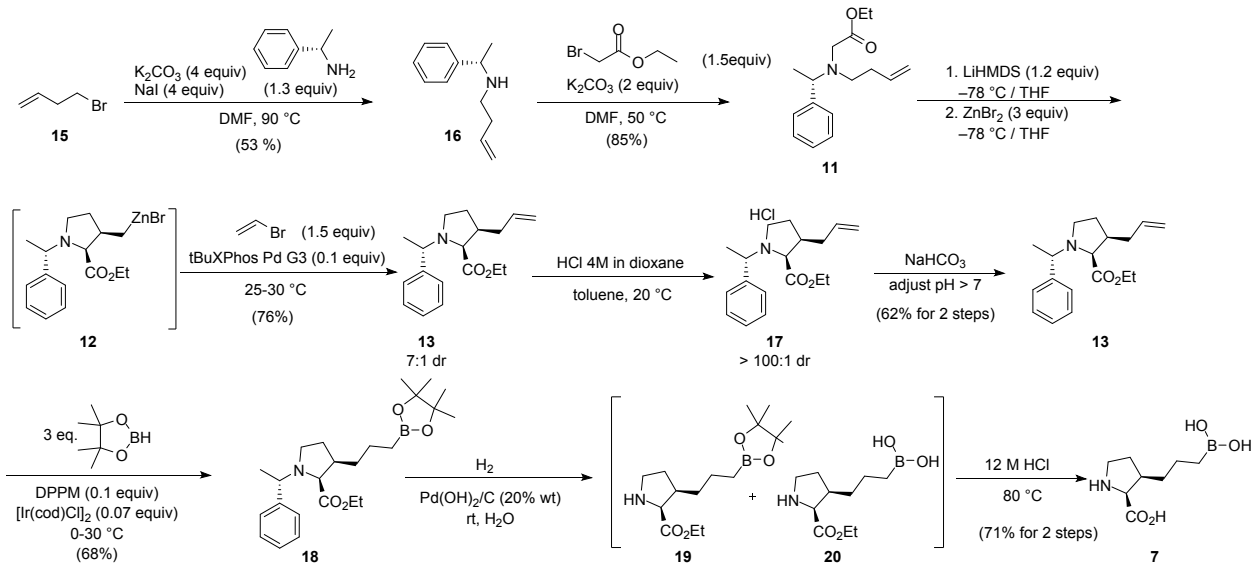

Scheme 4. Optimized Synthetic Route

Conclusion

In summary, we developed an efficient synthesis to 2,3-*cis* substituted pyrrolidine **7**. This route features a Zn-mediated cyclization that provided the desired *cis* configuration in high yield and dr. Our transition state model suggests a Zn-arene interaction and methyl-

methylene repulsion are important interactions for dictating the diastereoselectivity. In situ monitoring enabled high conversion and selectivity for this step. Key to the stereochemical purity of this route was the crystallization of the HCl salt **17** in toluene, which provided a diastereomeric upgrade from 87:13 dr to greater than 100:1. The final API was purified by ion-exchange chromatography in 10.2% overall yield and analyzed by LCMS with CAD detection and both ^{1}H and ^{11}B NMR. The chiral purity was verified by SFC. IEC used in the purification of **7** can be substituted for a crystallization from IPA / H_2O. This compares favorably to the previous route, which was 3.8% yield from an advanced intermediate.

EXPERIMENTAL SECTION

Materials and Methods. Reactions were performed in scintillation vials with Teflon septa and kept under a nitrogen atmosphere via a needle unless otherwise specified. Reactions were monitored by liquid chromatography/mass spectrometry (LCMS) or thin-layer chromatography (TLC) on silica gel 60 F254 plates (EMD) and visualized with UV light

(254 nm). IR spectra were obtained using a Metler Toledo ReactIR15 equipped with a diamond probe and a sampling rate of 1 scan/min (3000 to 650 cm^{-1}). The data was processed with iC IR 7.0 with standard background subtraction techniques. Flash chromatography was performed using prepacked RediSep Rf Gold silica gel columns on a Teledyne Isco CombiFlash Rf automated chromatography system. Organic solutions were concentrated under reduced pressure on a rotary evaporator. Tetrahydrofuran (THF), acetonitrile (MeCN), dimethylformamide (DMF), 1.0 M LiHMDS solution in THF, 4M HCl solution in dioxane were purchased from Sigma-Aldrich in Sure-Seal bottles and used as received. $ZnBr_2$ ampules (99.999%, beads, 10 mesh) were purchased from Sigma-Aldrich and stored in an inert atmosphere glovebox. For large scale reactions $ZnBr_2$ (>98%) was purchased from Sigma-Aldrich and dried under vacuum overnight at 80 °C before use. Precatalysts tBuXPhos Pd G3 and CPhos Pd G4 as well as $[Ir(COD)Cl]_2$ were purchased from Strem Chemicals and used as received.

Negishi Catalyst Screen. For this screen two kits containing 24 ligands each were used. An internally prepared ligand kit (prepared as described below) was used as well as a

commercially available cross-coupling kit (KitAlysis-24PD, Sigma-Aldrich). The experiments were set up in an MBraun glovebox (oxygen typically <5ppm). Liquid chemicals and reagent solutions were dosed using a micropipetter. Stirring was accomplished with parylene stir bars and a tumble stirrer.

Internal Ligand Kit. Ligands (0.25 μmol) were dosed into the reactor vials as solutions, and the solvent was removed by evacuation on a Genevac evaporator. A parylene stir bar was added to each vial, and the plates were stored in the glovebox or a desiccator. The 24 microvials containing the precatalysts were placed in an aluminum block. In a flask, a mixture of **12** was freshly prepared (0.158 M, 3 mL), then combined with 0.7 mL of vinyl bromide (1.0 M in THF) in a glovebox and 25 μL was dispensed into each of the precatalysts on the plate. Below each reactor vial in the aluminum 24-well plate was a 0.062 mm-thick silicon rubber gasket. Directly above the glass vial reactor tops was a 0.002 mm Teflon perfluoroalkoxy copolymer resin (PFA) sealing gasket, and above that were two more 0.062 mm-thick silicon rubber gaskets. The entire assembly was compressed between an aluminum top and the reactor base with nine evenly placed

screws. The reaction block was removed from the glovebox and placed on a tumble stirrer. The tumble stirrer was set to 50% and left at room temperature for 18 h. The reaction block was removed, and each sample was quenched by the addition of 100 µL of quenching solution (prepared by mixing 30.8 mg of biphenyl, 100 mL of MeCN, and 33 mL of DMSO). The plate was then resealed and stirred for 20 min. For analysis, a sample was removed from each reaction vial (25 µL) and diluted with 400 µL of MeCN. The diluted mixture was filtered and analyzed by LCMS.

KitAlysis Ligand Kit. In a flask, a mixture of **12** was freshly prepared (0.158 M, 3 mL), then combined with 0.7 mL of vinyl bromide (1.0 M in THF). In a glovebox 100 µL of the solution was charged to each of the vials in the kit. The plate was sealed as above, and the reaction block removed from the glovebox and placed on the tumble stirrer. The tumble stirrer was set to 50% and left at room temperature for 18 h. The reaction block was removed, and each sample was quenched by the addition of 400 µL of quenching solution (prepared by mixing 30.8 mg of biphenyl, 100 mL of MeCN, and 33 mL of DMSO). The plate was then resealed and stirred for 20 min. For analysis, a sample was removed

from each reaction vial (25 μL) and diluted with 400 μL of MeCN. The diluted mixture was filtered and analyzed by LCMS.

General Procedures. *(S)-N-(1-phenylethyl)but-3-en-1-amine* (**16**). Into a 5-L 4-necked round-bottom flask purged and maintained with an inert atmosphere of nitrogen, was placed 4-bromobut-1-ene (250.00 g, 1.85 mol, 1.00 equiv) in DMF (2.5 L), (1*S*)-1-phenylethan-1-amine (291.73 g, 2.40 mol, 1.30 equiv), K_2CO_3 (1.03 kg, 7407 mmol, 4.00 equiv) and sodium iodide (1.11 kg, 7.40 mol, 4.00 equiv). The resulting solution was stirred for 16 h at 90 ℃. The reaction mixture was then cooled to room temperature and quenched by the addition of water (2.50 L). The solution was transferred to a separatory funnel and extracted with 3 x 1000 mL of ethyl acetate. The organic layer was washed with 3 x 1000 mL of 5 % NaCl and dried over anhydrous magnesium sulfate. The solids were filtered out. The crude product was purified by distillation under reduced pressure (0.01 atm) and the product-bearing fraction was collected at 85 ℃. This resulted in 172.0 g (53%) of *(S)-N-(1-phenylethyl)but-3-en-1-amine* as a yellow oil. The spectroscopic data matched that reported in the literature.[20]

Ethyl (S)-N-(but-3-en-1-yl)-N-(1-phenylethyl)glycinate (**11**). Into a 5-L 4-necked round-bottom flask purged and maintained with an inert atmosphere of nitrogen, was placed (but-3-en-1-yl)[(1*S*)-1-phenylethyl]amine (172.00 g, 981.3 mmol, 1.00 equiv) in DMF (1.7 L), ethyl 2-bromoacetate (245.82 g, 1.472 mol, 1.50 equiv), K_2CO_3 (273.22 g, 1.963 mol, 2.00 equiv). The resulting solution was stirred for 16 h at 50 ℃. The reaction mixture was then cooled to room temperature and quenched by the addition of water (1.7 L). The mixture was transferred to a separatory funnel and extracted with 3 x 1000 mL of ethyl acetate. The organic layer was washed with 2 x 1000 mL of 5% NaCl and dried over anhydrous magnesium sulfate. The solids were filtered out and the filtrate was concentrated under reduced pressure. The residue was applied onto a silica gel column with ethyl acetate/petroleum ether (1:10). This resulted in 220.0 g (85%) of *Ethyl (S)-N-(but-3-en-1-yl)-N-(1-phenylethyl)glycinate* as yellow oil. The spectroscopic data matched that reported in the literature.[20]

Ethyl (2S,3R)-3-allyl-1-((S)-1-phenylethyl)pyrrolidine-2-carboxylate (**13**). Into a 10-L 4-necked round-bottom flask purged and maintained with an inert atmosphere of argon for

1 h, was placed ethyl 2-[(but-3-en-1-yl)[(1*S*)-1-phenylethyl]amino]acetate (**11**) (220.00 g, 841.7 mmol, 1.00 equiv) in 2.2 L dry THF (H_2O < 0.01%). The mixture was cooled to –78 ℃, and LiHMDS (1.00 L, 1 mol/L, 1.2 equiv) was added. The solution was stirred at –78 ℃ for 10 min and then allowed to warm to 0 ℃ and stirred at 0 ℃ for 30min. An aliquot of the reaction mixture was quenched with D_2O and analyzed by LCMS to show that the reaction (enolate formation) was complete. The solution of the lithium enolate was cooled back down to –78 ℃. In a separate flask, $ZnBr_2$ (568.65 g, 2.52 mol, 3.00 equiv) was dissolved in THF (1.50 L) and 284 g of 4Å-molecular sieves was added. The solution of $ZnBr_2$ was added into the solution of the lithium enolate at –78 ℃ over 30 min (exotherm observed). The solution was warmed to rt and stirred at rt for 1 h. An aliquot of the reaction mixture was quenched with D_2O (**11** and **14** have the same mass) and analyzed by LCMS to show that the reaction (conversion of **11** to **12**) was complete. To the mixture was added vinylbromide in THF (1.263 L, 1.263 mol, 1.50 equiv 1 mol/L) (dried with 4Å-molecular sieves (43 g)) dropwise at 25 ℃ over 10 min. t-BuXPhos Pd G3 (66.86 g, 84.173 mmol, 0.10 equiv) was added into the mixture at 25 ℃, and the mixture was stirred at 30 ℃ for 16 h. The reaction mixture was cooled to 0 ℃ with a water/ice bath and was

quenched by addition of 1000 mL of HCl (1M). The resulting solution was transferred to a separatory funnel and extracted with 3 x 1000 mL of ethyl acetate. The organic layer was washed with 2 x 500 mL of 10% $NaHCO_3$. The organic layer was dried over anhydrous magnesium sulfate. The solids were filtered off and the filtrate was concentrated under reduced pressure. The residue was applied onto a silica gel column with ethyl acetate/petroleum ether (1:10). This resulted in 220.0 g (76%) of ethyl (2*S*,3*R*)-1-[(1*S*)-1-phenylethyl]-3-(prop-2-en-1-yl)pyrrolidine-2-carboxylate as a light yellow oil with of 7:1. Major diastereomer: ^{1}H NMR (600 MHz, $CDCl_3$) δ 7.39 (s, 5H), 5.63 (m, 1H), 5.01 (d, *J* = 4.6 Hz, 1H), 4.99 (s, 1H), 4.46 (s, 1H), 4.22 (s, 1H), 4.09 (m, 1H), 3.85 (d, *J* = 7.2 Hz, 1H), 3.56 (s, 1H), 2.83 (s, 1H), 2.35 (s, 1H), 2.13 (dt, *J* = 12.4, 6.0 Hz, 1H), 1.88 (dq, *J* = 11.6, 7.1 Hz, 1H), 1.80 (m, 1H), 1.74 (d, *J* = 6.9 Hz, 1H), 1.15 (t, *J* = 7.1 Hz, 1H). ^{13}C NMR (600 MHz, $CDCl_3$) δ 13.92, 19.89, 28.81, 34.38, 40.89, 52.32, 61.79, 64.25, 66.40, 117.49, 129.13, 129.70, 134.47, 136.13, 168.32. Two peaks coincidentally overlap.

Ethyl (2S,3R)-3-allyl-1-((S)-1-phenylethyl)pyrrolidine-2-carboxylate hydrochloride (**17**). Into a 3-L 4-necked round-bottom flask purged and maintained with an inert atmosphere

of nitrogen, was placed crude ethyl (2*S*,3*R*)-1-[(1*S*)-1-phenylethyl]-3-(prop-2-en-1-yl)pyrrolidine-2-carboxylate (205.00 g, 713.3 mmol, 1.00 equiv) in toluene (1000 mL). HCl (200 mL, 4M in 1,4-dioxane) was added to the mixture at 20 ℃ over 10 min. The resulting solution was stirred for 5 hours at room temperature. The solids were collected by filtration (**13**:**13A** = 1:1 in mother liquor). The solids (dr = 97:3) were slurried with *n*-hexanes (5 volumes) for 2 h, and were collected by filtration. This resulted in 140 g of ethyl (2*S*,3*R*)-1-[(1*S*)-1-phenylethyl]-3-(prop-2-en-1-yl)pyrrolidine-2-carboxylate hydrochloride as a white solid (61%, dr =99.7:0.3). ^{1}H NMR (400 MHz, $CDCl_3$) δ 13.26 (s, 1H), 7.65 (s, 2H), 7.37 (s, 3H), 5.70 – 5.51 (m, 1H), 5.02 – 4.96 (m, 1H), 4.95 (s, 1H), 4.45 (p, *J* = 6.9 Hz, 1H), 4.05 (dddt, *J* = 18.0, 10.8, 7.2, 3.6 Hz, 3H), 3.79 (dd, *J* = 7.1, 4.1 Hz, 1H), 3.50 (tdd, *J* = 10.9, 6.6, 3.8 Hz, 1H), 3.23 – 3.07 (m, 1H), 2.35 (ddd, *J* = 12.3, 3.7 Hz, 1H), 2.11 (dt, *J* = 13.7, 6.0 Hz, 1H), 1.90 (dd, *J* = 11.6, 7.3 Hz, 1H), 1.83 (d, *J* = 6.9 Hz, 4H), 1.81 – 1.68 (m, 1H), 1.12 (t, *J* = 7.2 Hz, 3H).

Ethyl (2S,3R)-3-allyl-1-((S)-1-phenylethyl)pyrrolidine-2-carboxylate (**13**) from *Ethyl (2S,3R)-3-allyl-1-((S)-1-phenylethyl)pyrrolidine-2-carboxylate hydrochloride* (**17**). Into a

1-L 3-necked round-bottom flask purged and maintained with an inert atmosphere of nitrogen, was placed ethyl (2*S*,3*R*)-1-[(1*S*)-1-phenylethyl]-3-(prop-2-en-1-yl)pyrrolidine-2-carboxylate hydrochloride (55 g, 0.17 mol) in CH_2Cl_2 (165 mL). $NaHCO_3$ (10 %) was added into the mixture to adjust the pH=9. The solution was extracted with 2 x 200 mL of CH_2Cl_2. The organic layer was washed with 2 x 200 mL brine and dried over anhydrous magnesium sulfate. The solids were filtered out and the solution was concentrated under reduced pressure. This resulted in 48.8 g (quantitative) of ethyl (2*S*,3*R*)-1-[(1*S*)-1-phenylethyl]-3-(prop-2-en-1-yl)pyrrolidine-2-carboxylate as light yellow oil.

Ethyl(2S,3R)-1-((S)-1-phenylethyl)-3-(3-(4,4,5,5-tetramethyl-1,3,2-dioxaborolan-2-yl)propyl)pyrrolidine-2-carboxylate (**18**). Into a 1-L 3-necked round-bottom flask purged and maintained with an inert atmosphere of nitrogen, was placed ethyl (2*S*,3*R*)-1-[(1*S*)-1-phenylethyl]-3-(prop-2-en-1-yl)pyrrolidine-2-carboxylate (61.00 g, 212.2 mmol, 1.00 equiv) in CH_2Cl_2 (610mL), $[Ir(cod)Cl]_2$ (9.98 g, 14.9 mmol, 0.07 equiv), DPPM (8.16 g, 21.2 mmol, 0.10 equiv) and 4Å-molecular sieves (61 g). The mixture was stirred for 30 min at 25 ℃. 4,4,5,5-tetramethyl-1,3,2-dioxaborolane (81.49 g, 636.7 mmol, 3.00 equiv)

was added into the mixture at 0 ℃. The solution was stirred at 30 ℃ for 4h. The reaction was then quenched by the addition of 100 mL of water at 0 ℃. The mixture was transferred to a separatory funnel and extracted with 2 x 200 mL of CH_2Cl_2. The organic layer was washed with brine and dried over anhydrous magnesium sulfate. The solids were filtered, and the filtrate was concentrated under reduced pressure. The residue was purified by silica gel chromatography with ethyl acetate/petroleum ether (1:5). This resulted in 60 g (68.1%) of ethyl (2*S*,3*R*)-1-[(1*S*)-1-phenylethyl]-3-[3-(4,4,5,5-tetramethyl-1,3,2-dioxaborolan-2-yl)propyl]pyrrolidine-2-carboxylate as a light yellow oil. ^{1}H NMR (600 MHz, DMSO-d_6) δ 7.29 (m, 2H), 7.22 (m, 3H), 4.03 (q, *J*= 7.2 Hz, 1H), 3.99 (tt, *J* = 7.1, 3.5 Hz, 1H), 3.62 (q, *J* = 6.5 Hz, 1H), 3.22 (d, *J* = 7.9 Hz, 1H), 2.88 (t, *J* – 7.0 Hz, 2H), 2.21 (m, 1H), 1.94 (ddd, *J* = 7.7, 5.2, 3.6 Hz, 1H), 1.48 (m, 1H), 1.23 (d, *J* = 6.6 Hz, 3H), 1.17 (t, *J* = 7.2 Hz, 2H),1.14 (s, 12H), 1.12 (t, *J* = 7.1 Hz, 3H), 1.04 (m, 1H), 0.59 (t, *J* = 7.6 Hz, 2H).

Mixture of ethyl (2S,3R)-3-(3-(4,4,5,5-tetramethyl-1,3,2-dioxaborolan-2-yl)propyl)pyrrolidine-2-carboxylate (**19**) and *(3-((2S,3R)-2-(ethoxycarbonyl)pyrrolidin-3-*

yl)propyl)boronic acid (**20**). Into a 2-L round-bottom flask, was placed ethyl (2*S*,3*R*)-1-[(1*S*)-1-phenylethyl]-3-[3-(4,4,5,5-tetramethyl-1,3,2-dioxaborolan-2-yl)propyl]pyrrolidine-2-carboxylate (25 g) in water (500 mL) and 20% wt $Pd(OH)_2$/C (10 g). The mixture was placed under an atmosphere of hydrogen gas. The resulting suspension was stirred for 40 h at room temperature. The solids were filtered out and the filtrate was concentrated under reduced pressure. The reaction was repeated in a second batch. This resulted in 40 g (crude) mixture of ethyl (2*S*,3*R*)-3-[3-(4,4,5,5-tetramethyl-1,3,2-dioxaborolan-2-yl)propyl]pyrrolidine-2-carboxylate and [3-[(2*S*,3*R*)-2-(ethoxycarbonyl)pyrrolidin-3-yl]propyl]boronic acid.

(2S,3R)-3-(3-boronopropyl)pyrrolidine-2-carboxylic acid (**7**). Into a 1-L round-bottom flask, was placed a mixture of ethyl (2*S*,3*R*)-3-[3-(4,4,5,5-tetramethyl-1,3,2-dioxaborolan-2-yl)propyl]pyrrolidine-2-carboxylate and [3-[(2*S*,3*R*)-2-(ethoxy carbonyl) pyrrolidin-3-yl]propyl]boronic acid (40 g) in 12 M HCl (, 220 mL). The mixture was stirred and heated to 80 ℃ for 16 h. The mixture was monitored by HPLC using CAD and MS detectors. Upon completion, the mixture was concentrated to a solid at 40 ℃ under vacuum, and

redissolved in water (80 mL). The resulting solution was washed with 5 x 100 mL CH_2Cl_2. The aqueous layer was collected and concentrated at 40 ℃ under vacuum to give a yellow oil. A Dowex 50WX8 200-400 (H) resin (400 g) column was washed with 3 x 200 mL water to adjust pH~ 7. The yellow oil was dissolved in 40 mL of H_2O and applied on the Dowex column. The column was washed with 5 x 200 mL pure water until the pH of the eluent was ~7. Then 2 x 200 mL NH_4OH (6%) was added on the column to elute the desired product. The collected solution was concentrated at 40 ℃ to get 16.0 g of a foam corresponding to (2*S*,3*R*)-3-(3-boronopropyl)pyrrolidine-2-carboxylic acid with LCAP 97% and containing 2.6% of compound **20**. The desired compound was further purified by crystallization using 10 volumes of an 8:1 (v:v) IPA:H_2O mixture; after stirring for 16 h at 25 ℃, the solid was collected by filtration giving 14.5 g (64% over two steps) of (2*S*,3*R*)-3-(3-boronopropyl)pyrrolidine-2-carboxylic acid as a white solid. ^{1}H NMR (300 MHz, D_2O) δ 4.05 (d, *J* = 7.9 Hz, 1H), 3.46 (dd, *J* = 12.2, 5.8 Hz, 1H), 3.26 (dt, *J* = 11.6, 7.7 Hz, 1H), 2.50 (d, *J* = 6.9 Hz, 1H), 2.14 (dd, *J* = 13.3, 6.9 Hz, 1H), 1.78 (dd, *J* = 13.3, 6.9 Hz, 1H), 1.68 – 1.29 (m, 3H), 1.17 (d, *J* = 10.3 Hz, 1H), 0.76 (q, *J* = 7.7 Hz, 2H). ^{11}B NMR (96 MHz, D_2O) δ 33.19.

Supporting Information. NMR spectra, computational methods, and additionall figures can be found in the Supporting Information, available free of charge on the ACS Publications website at DOI:

AUTHOR INFORMATION

Corresponding Author

*To whom correspondence should be addressed: thomas.lyons@merck.com.

Present Addresses

‡T.A.M.: Infinity Pharmaceuticals, Inc., 1100 Mass Ave, Cambridge, MA 02138.

Author Contributions

The manuscript was written through contributions of all authors. All authors have given approval to the final version of the manuscript.

Notes

The authors declare no competing financial interest.

ACKNOWLEDGMENT

The authors would like to acknowledge Emily Corcoran, Michael Ardolino, Aaron Sather, Matthew Maddess, and L.C. Campeau for helpful advice during the preparation of this manuscript. The authors would also like to acknowledge Josep Sauri, Jingjun Yin, Licheng Song, and Juajie Zhang for helpful discussions and assistance with experiments.

ABBREVIATIONS

LCAP, liquid chromatography area percent; LCMS, liquid chromatography mass spectrometry; CAD, charged aerosol detection; TS, transition state; equiv, equivalents; dr, diastereomeric ratio; ARG, Arginase; LDA, lithium diisopropylamide; LiHMDS, lithium bis(trimethylsilyl)amide; KHMDS, potassium bis(trimethylsilyl)amide; THF, tetrahydrofuran; SFC, supercritical fluid chromatography; DPPM, 1,1-bis(diphenylphosphino)methane; CPhosPd-G4, 2-dicyclohexylphosphino-2',6'-bis(*N,N*-dimethylamino)biphenyl fourth generation (G4) Buchwald precatalyst; APhosPd-G2, Chloro[4-(di-tert-butylphosphino)-N,N-dimethylaniline-2-(2′-aminobiphenyl)]palladium(II) second generation (G2) Buchwald Pd precatalyst; DTBPF-G3, 1,1'-bis(di-*tert*-

butylphosphino)ferrocene (G3) third generation Buchwald Pd precatalyst; tBuXPhos-G3, 2-di-*tert*-butylphosphino-2',4',6'-triisopropylbiphenyl (G3) third generation Buchwald Pd precatalyst; SM, starting material; IPA, isopropanol.

REFERENCES

1. Christianson, D. W.; Cox, J. D., Catalysis by metal-activated hydroxide in zinc and manganese metalloenzymes. *Annu. Rev. Biochem.* **1999,** *68*, 33-57.
2. Ash, D. E.; Cox, J. D.; Christianson, D. W., *Arginase: A binuclear manganese metalloenzyme*. 2000; Vol. 37, p 407-428.
3. Morris, S. M., Regulation of enzymes of the urea cycle and arginine metabolism. *Annu. Rev. Nutr.* **2002,** *22*, 87-105.
4. Raber, P.; Ochoa, A. C.; Rodriguez, P. C., Metabolism of L-Arginine by Myeloid-Derived Suppressor Cells in Cancer: Mechanisms of T cell suppression and Therapeutic Perspectives. *Immunol. Invest.* **2012,** *41*, 614-634.
5. Singh, R.; Pervin, S.; Karimi, A.; Cederbaum, S.; Chaudhuri, G., Arginase activity in human breast cancer cell lines: N-omega-hydroxy-L-arginine selectively inhibits cell proliferation and induces apoptosis in MDA-MB-468 cells. *Cancer Res.* **2000,** *60*, 3305-3312.
6. Ino, Y.; Yamazaki-Itoh, R.; Oguro, S.; Shimada, K.; Kosuge, T.; Zavada, J.; Kanai, Y.; Hiraoka, N., Arginase II expressed in cancer-associated fibroblasts indicates tissue hypoxia and predicts poor outcome in patients with pancreatic cancer. *PLoS One* **2013,** *8*, e55146.
7. Miret, J. J.; Kirschmeier, P.; Koyama, S.; Zhu, M.; Li, Y. Y.; Naito, Y.; Wu, M.; Malladi, V. S.; Huang, W.; Walker, W.; Palakurthi, S.; Dranoff, G.; Hammerman, P. S.; Pecot, C. V.; Wong, K.-K.; Akbay, E. A., Suppression of Myeloid Cell Arginase Activity leads to Therapeutic Response in a NSCLC Mouse Model by Activating Anti-Tumor Immunity. *Journal for ImmunoTherapy of Cancer* **2019,** *7*, 32.
8. Gannon, P. O.; Godin-Ethier, J.; Hassler, M.; Delvoye, N.; Aversa, M.; Poisson, A. O.; Péant, B.; Alam Fahmy, M.; Saad, F.; Lapointe, R.; Mes-Masson, A.-M., Androgen-regulated expression of arginase 1, arginase 2 and interleukin-8 in human prostate cancer. *PloS one* **2010,** *5*, e12107-e12107.
9. Timosenko, E.; Hadjinicolaou, A. V.; Cerundolo, V., Modulation of cancer-specific immune responses by amino acid degrading enzymes. *Immunotherapy* **2017,** *9*, 83-97.
10. de Boniface, J.; Mao, Y.; Schmidt-Mende, J.; Kiessling, R.; Poschke, I., Expression patterns of the immunomodulatory enzyme arginase 1 in blood, lymph nodes and tumor tissue of early-stage breast cancer patients. *Oncoimmunology* **2012,** *1*, 1305-1312.

11. Rodriguez, P. C.; Quiceno, D. G.; Zabaleta, J.; Ortiz, B.; Zea, A. H.; Piazuelo, M. B.; Delgado, A.; Correa, P.; Brayer, J.; Sotomayor, E. M.; Antonia, S.; Ochoa, J. B.; Ochoa, A. C., Arginase I Production in the Tumor Microenvironment by Mature Myeloid Cells Inhibits T-Cell Receptor Expression and Antigen-Specific T-Cell Responses. *Cancer Res.* **2004,** *64*, 5839.
12. Steggerda, S. M.; Bennett, M. K.; Chen, J.; Emberley, E.; Huang, T.; Janes, J. R.; Li, W.; MacKinnon, A. L.; Makkouk, A.; Marguier, G.; Murray, P. J.; Neou, S.; Pan, A.; Parlati, F.; Rodriguez, M. L. M.; Van de Velde, L.-A.; Wang, T.; Works, M.; Zhang, J.; Zhang, W.; Gross, M. I., Inhibition of arginase by CB-1158 blocks myeloid cell-mediated immune suppression in the tumor microenvironment. *Journal for ImmunoTherapy of Cancer* **2017,** *5*, 101-101.
13. Stille, J. K., The Palladium-Catalyzed Cross-Coupling Reactions of Organotin Reagents with Organic Electrophiles [New Synthetic Methods (58)]. *Angew. Chem., Int. Ed.* **1986,** *25*, 508-524.
14. Pothukanuri, S. G., P.; Lloyd, J.; Finlay, H.; Adisechan, A. Pyrrolotriazines as potassium ion channel inhibitors WO2014/143606, 2014.
15. 2-3 steps from commercially available starting materials.
16. Ilies, M.; Di Costanzo, L.; Dowling, D. P.; Thorn, K. J.; Christianson, D. W., Binding of alpha,alpha-Disubstituted Amino Acids to Arginase Suggests New Avenues for Inhibitor Design. *J. Med. Chem.* **2011,** *54*, 5432-5443.
17. Vadon-Legoff, S.; Dijols, S.; Mansuy, D.; Boucher, J. L., Improved and high yield synthesis of the potent arginase inhibitor: 2(*S*)-mino-6-boronohexanoic acid. *Org. Process Res. Dev.* **2005,** *9*, 677-679.
18. Wang, D. S.; Chen, Q. A.; Lu, S. M.; Zhou, Y. G., Asymmetric Hydrogenation of Heteroarenes and Arenes. *Chem. Rev.* **2012,** *112*, 2557-2590.
19. Screening efforts to discover an enantioselective hydrogenation of pyrrole intermediate 3 were unsuccessful. Few examples of such a reaction have been reported and it remains an important challenge in catalysis. For related examples, see ref 18.
20. Karoyan, P.; Chassaing, G., Asymmetric synthesis of (2S,3S)- and (2S,3R)-3-prolinomethionines: 3-methylsulfanylmethyl-pyrrolidine-2-carboxylic acids. *Tetrahedron: Asymmetry* **1997,** *8*, 2025-2032.
21. Karoyan, P.; Chassaing, G., New strategy for the synthesis of 3-substituted prolines. *Tetrahedron Lett.* **1997,** *38*, 85-88.
22. Karoyan, P.; Quancard, J.; Vaissermann, J.; Chassaing, G., Amino−Zinc−Enolate Carbometalation Reactions: Application to Ring Closure of Terminally Substituted Olefin for the Asymmetric Synthesis of cis- and trans-3-Prolinoleucine. *J. Org. Chem.* **2003,** *68*, 2256-2265.
23. Lorthiois, E.; Marek, I.; Normant, J. F., Zinca-ene-allene and zinc-enolate cyclization. Towards the synthesis of polysubstituted pyrrolidines. *Tetrahedron Lett.* **1997,** *38*, 89-92.
24. Lorthiois, E.; Marek, I.; Normant, J. F., Diastereoselective and enantioselective intramolecular amino-zinc-enolate carbometalation reactions. A new polysubstituted pyrrolidines synthesis. *J. Org. Chem.* **1998,** *63*, 2442-2450.
25. Lorthiois, E.; Marek, I.; Normant, J. F., Amino zinc enolate carbocyclization reactions. New access to polysubstituted piperidine derivatives. *J. Org. Chem.* **1998,** *63*, 566-574.
26. Karoyan, P.; Triolo, A.; Nannicini, R.; Giannotti, D.; Altamura, M.; Chassaing, G.; Perrotta, E., Solid-phase amino-zinc-enolate cyclization for the synthesis of 3-substituted prolines. *Tetrahedron Lett.* **1999,** *40*, 71-74.

27. Denes, F.; Perez-Luna, A.; Chemla, F., Addition of Metal Enolate Derivatives to Unactivated Carbon-Carbon Multiple Bonds. *Chem. Rev.* **2010,** *110*, 2366-2447.
28. Kim, J. H.; Ko, Y. O.; Bouffard, J.; Lee, S.-g., Advances in tandem reactions with organozinc reagents. *Chem. Soc. Rev.* **2015,** *44*, 2489-2507.
29. Quancard, J.; Magellan, H.; Lavielle, S.; Chassaing, G.; Karoyan, P., Amino-zinc-ene-enolate cyclisation: a short access to (2*S*,3*R*)- and (2*S,*3*S*)-3-benzylprolines (3-benzylpyrrolidine-2-carboxylic acids). *Tetrahedron Lett.* **2004,** *45*, 2185-2187.
30. Déchamps, I.; Gomez Pardo, D.; Karoyan, P.; Cossy, J., Efficient Enantioselective Formal Synthesis of Ro 67-8867, a NMDA 2B Receptor Antagonist. *Synlett* **2005,** *2005*, 1170-1172.
31. Han, C.; Buchwald, S. L., Negishi Coupling of Secondary Alkylzinc Halides with Aryl Bromides and Chlorides. *J. Am. Chem. Soc.* **2009,** *131*, 7532-7533.
32. Yang, Y.; Niedermann, K.; Han, C.; Buchwald, S. L., Highly Selective Palladium-Catalyzed Cross-Coupling of Secondary Alkylzinc Reagents with Heteroaryl Halides. *Org. Lett.* **2014,** *16*, 4638-4641.
33. Isolation of the minor diastereomer revealed a cis-2R,3S configuration. No trans product was observed.
34. We speculate that small volumes and variable stirring rates led to this discrepancy in reactivity. The lack of solubility of the Zn-intermediate ultimately prevented us from pursuing this further.
35. Shevlin, M., Practical High-Throughput Experimentation for Chemists. *ACS Med. Chem. Lett.* **2017,** *8*, 601-607.
36. For simplicity, the methyl ester was used in the DFT experiments.
37. Dudev, T.; Lim, C., Tetrahedral vs Octahedral Zinc Complexes with Ligands of Biological Interest: A DFT/CDM Study. *J. Am. Chem. Soc.* **2000,** *122*, 11146-11153.
38. The translational entropy loss upon coordination of ether molecules is accounted for by including the solution reaction to the activation free energy of the solvent cage, where the ether concentration is 13.5 M instead of 1 M, and a ~1.5 kcal/mol correction is applied.
39. Additional development could focus on protecting group screens and isolation strategies that would eliminate the need for chromatography.